THE UNIVERSITY OF MICHIGAN
DEPARTMENT OF MECHANICAL ENGINEERING
CAVITATION AND MULTIPHASE FLOW LABORATORY

Report No. UMICH 014571-3-T

INVESTIGATION OF THE BEHAVIOR OF THIN LIQUID FILM WITH CO-CURRENT STEAM FLOW

(Submitted to Two-Phase Flow and Heat Transfer Symposium - Workshop, Ft. Lauderdale, Florida, October 18-20, 1976)

W. Kim
S. Krzeczkowski
F. G. Hammitt

Supported by: National Science Foundation Grant No. ENG 75-2315 and National Academy of Sciences (with cooperative program with the Polish Academy of Sciences)

July, 1976

List of Tables

List of Figures

1. Introduction

Film flow is a special case of two-phase flow, which is more amenable to detailed study than are most other types of two-phase flow. Furthermore, a detailed knowledge of the phenomena occurring in film flow would assist greatly in understanding many of the more complex types of two-phase flow and the mechanisms of heat and mass transfer in such flow.

The occurrence and applications of film flow in modern technology are numerous and important, for example, steam turbine blades, the conveying of liquids by co-current gas streams in oil pipelines, boiler tubes, and heat transfer from wavy films of molten material on spacecraft.

For the modern large powerplants, the behavior and stability of thin liquid films on the turbine blades under high velocity steam flow and their subsequent break-up into liquid droplets, which are then entrained into the wake and give rise to an erosion problem in the next downstream rotating row have come to the attention of many researchers, and have been considered to involve important economic factors. Along these lines of interest, a wet steam tunnel has been designed, constructed and tested at the University of Michigan (1,2,3,4,5).

The low pressure steam tunnel can produce approximately sonic velocity ($\sim$ 450 m/sec) in a rectangular test section (8 cm x 8 cm) at a pressure of $\sim$ 3 psia ($\sim$ 20.67 x $10^3 N/m^2$). Simulated turbine blades, i.e., essentially thin flat plates, are inserted parallel to the flow direction along the axis of the test section.

Liquid film thickness measurement techniques using electrical-conductivity gages have been developed and calibrated (2,3). The behavior of the liquid film, under adiabatic and diabatic conditions, has been reported. (5) Most recently, liquid droplet structure and population distribution in the steam flow have been studied by making use of high-speed photographic technique (4).

In this paper , we are particularly interested in film stability, especially regarding the wave patterns appearing at the interface between film and steam surface. We have measured the wave lengths and film thicknesses under diabatic conditions for various steam and liquid flow rates. From these data, a kind of transition map (from symmetric waves to non-symmetric wave clusters, etc.) is presented. Standard deviation of the individual waves from the mean wave length is calculated, giving some measure of the randomness of the wave patterns in each regime of the map.

2. Experimental Apparatus and Condition

Figure 1 shows a schematic diagram of our steam tunnel facility. The test section is composed of a horizontal rectangular plexiglas test section with the blade inserted parallel to the stream (Fig. 2). The liquid film thickness measurement technique is reported elsewhere (2,eg.) and is not discussed here.

As was discussed in Ref. 5, the steam flow rate was measured by an upstream orifice rather than a pitot tube, This was not used because of its contribution to turbulence. The liquid film is formed by supplying the liquid through a slot in the blade instead of by condensing the steam. The liquid flow rate is measured by a conventional flow meter.

The liquid film behavior and stability are investigated by

means of a high-speed camera with a strobe flash unit as light source. By visual inspection of the photos, information about the stability of the liquid film was obtained (eg. wave patterns, wave lengths, and liquid film break-up and shedding). The oscilloscope pictures, which give the film thickness and frequency information, were taken simultaneously with the high-speed camera picture by connecting a syncronization unit between the two cameras.

The range of this investigation is characterized by the following conditions: steam velocity - 50 m/s to 300 m/s.

liquid film flow- 0.005 cm^3/sec.cm to 0.2 cm^3/sec.cm (per unit of width)

mean film thickness - 20 μm to 220 μm

wave lengths (*symmetric wave - 0.5 mm to 2.5 mm
non-symmetric wave - 5 mm to 10 mm)

3. General Observation of Wave Patterns

For a constant steam velocity, we can observe the following wave phenomena as we increase the liquid flow rate. At very low liquid flow rates, dry patches (Fig. 3), and/or rivulets (14), have been observed. These are presumably due to surface tension and shear stress. At a slightly larger liquid flow rate, small symmetrical waves appear ($\lambda = 1 \sim 2.5$ mm). The wave fronts are almost straight and perpendicular to the direction of the flow (Fig. 4,5). As the flow rate increases the wave lengths tend to be smaller (Fig. 12).

At still larger flow rates, the regular symmetrical waves tend to become less regular and the cross-section of the wave assumes the non-symmetrical shape of a cluster with a steep front and a long tail (Fig. 6,7,8). Usually each cluster wave is preceded by a number of satellite wavelets (termed "push-waves") by Wurz (13,15) which move as a group with the main wave (8). The wave length of this cluster

*The terms "symmetric and non-symmetric" are explained later.

wave was ~ 5-10 mm and that of the wavelets are ~ 0.3-0.4 mm mm. The wave lengths of these cluster waves become less as the flow rate increases (Fig. 12). However, the variation of the wave lengths of the satellites were not precisely detected since they were too small for the camera system used.

In this regime of flow the wave fronts show a tendency to form bulges, to split or to overtake each other. As the liquid flow rate is increased, a stage is reached where the main waves and their accompanying satellites have become so randomly mixed that the individual wave fronts can hardly be distinguished, and the surface breaks and sheds into the steam flow. (Fig. 9,10, 11).

4. Results

Tailby and Portalski (10) have reported measurements of the wave lengths near the point of wave inception on vertical films of various liquids. For most flow rates, the wave length in the region away from the line of inception varies considerably with time. However, it is possible to obtain a mean wave length by averaging the distances between fronts of a large number of waves. As is seen in Fig. 12, the wave length decreases with increasing liquid flow rate. There is then a marked increase in the mean wave length in the non-symmetric cluster wave regime (Fig. 13). The ratio $\lambda^{Non-sym}_{mean} / \lambda^{Sym}_{mean}$ is 5, where λ^{Sym}_{mean} is mean wave length of the symmetric wave and $\lambda^{non-sym}_{mean}$ is mean wave length of the non-symmetric cluster wave. Then again the wave length decreases as the liquid flow rate increases.

Mean wave lengths and standard deviation of the individual waves from them are given in Table 1. Apparently in the symmetric wave regime, the wave lengths are comparatively regular and in the non-symmetric cluster wave regime, the waves are quite scattered, i.e. the standard deviation is increased by 6x.

No reliable dimensionless parameters have been found so far for the critical or transitional behavior of the wave patterns, especially for this particular steam-liquid flow case. However, Fig. 13, is a dimensionless diagram showing that the value of the maxima $(\frac{\lambda}{h})$ is increased with increased steam velocity, but is less dependent on increased liquid flow rate.

Perhaps the most essential part of the paper is the transition "map " presented in Fig. 14. Many such transition maps have been presented by other authors (11,12,13). However, all of these are for liquid film and air instead of liquid film and steam as in the present case. This flow regime is in fact much more complicated because of heat and mass transfer, the mechanism of which is not thoroughly known at this time.

The explanations for the "map" (Fig. 14) follow.

Regime I: As is seen in Fig. 3 dry patches and rivulets predominate. These are of importance in safety studies of liquid-cooled nuclear reactors (either liquid metal or water). A theoretical study (14) has been done for the case of gravity-driven liquid flow.

Regime II: Symmetrical 2-dimensional waves are observed (Fig. 4,5).

Regime III: Transition region to non-symmetric cluster waves.

Regime IV: Mainly non-symmetric cluster waves (Fig. 6,7,8).

Regime V: The region where crests of the cluster waves are torn away into droplets (Fig. 8,9,10).

In Figure 15 the transition line between IV and V is compared with the results of various previous investigators (13,e.g.) In all cases the gas flows are air. In our steam-liquid film study the liquid film was torn when it was of $\sim$0.2 x thickness and at the gas phase velocity of the air-liquid film case. In Regime III wave lengths increase rapidly. The mechanisms of these transitions are of great interest, and will be studied in more detail in the future.

5. Conclusions

The object of this investigation was to study the behavior of injected thin films of water under the effect of steam flow with moderate to high subsonic velocity. The wave lengths were measured by high-speed photography. A plot of wave lengths under different steam flow and liquid flow conditions indicates that wave lengths decrease as liquid flow rates increase but increase as steam velocities decrease.

The mean wave lengths and standard deviations are listed (Table 1). This gives the measure of the randomness of the wave lengths in symmetric and non-symmetric waves. A "transition map" for liquid film-steam flow is presented. The mechanisms of the transition lines will be the subject of future study.

Compared with an air-liquid film transition map previously published (13), we have found that our steam-liquid film flow is broken and torn away at less thickness, and at higher steam velocity, than was observed for the air-water studies.

The results so far obtained are particularly suitable for describing the limits associated with the formation of waves and droplets, which are important from the viewpoint of damage in large steam turbines.

References

1. J. Krzyzanowski, "Wet-Steam Tunnel Facility - Design and Program of Investigations," ORA Report No. UMICH 03371-18-T, June 1972.

2. J. Mikielewicz, F.G. Hammitt, "Generalized Characteristics of Electrical Conductance Film Thickness Gauges," ORA Report No. UMICH 012449-7-I, December 1974.

3. F.G. Hammitt, J. Mikielewicz, G. Ernst, "Steam Tunnel Initial Operation and Results," ORA Report No. UMICH 012449-6-T, January 1975.

4. S. Krzeczkowski, W. Kim, F.G. Hammitt, J-B. Hwang, "Investigations of Secondary Liquid Phase Structure in Steam Wake," ORA Report No. UMICH 014571-1-T, June 1976.

5. F.G. Hammitt, J-B. Hwang, etal., "Liquid Film Thickness Tests - Wet Steam Tunnel," ORA Report No. UMICH 012449-9-T, June 1975.

6. A.E. Duckler, M. Wicks, Modern Chemical Engineering, 1, Reinhold, New York, 1963, p. 349-435.

7. D.S. Scott, Advanced Chemical Engineer, 4, 1963, p. 199.

8. P.G. Mayer, J. Hydraulics Div., ASCE, 85, (HY7), 1959, p. 99.

9. A. Mancuso, F.G. Hammitt, etal., "Data Reduction Procedure - Steam Tunnel Film Thickness Tests," ORA Report No. UMICH 012449-20-I-A, June 1975.

10. S.R. Tailby, S. Portalski, Trans. Inst. Chem. Engrs. (London), 40, 1962, p. 114.

11. Y. Taitel, A.E. Duckler, "A Model for Prediction Flow Regime Transitions in Horizontal and Near-Horizontal Gas-Liquid Flow," AIChE J., 22, 1976, p.47-55.

12. O. Baker, "Simultaneous Flow of Oil and Gas," Oil Gas J., 53, July 1954, p. 185.

13. D. Wurz, "Flow Behavior of Thin Water Films Under the Effect of Co-current Air Flow of Moderate to High Subsonic Velocities," Proc. 3rd International Conf. Rain Erosion and Associated Phenomena, Aug. 11-12, 1970, ed. A.A. Fyall, Royal Aircraft Estab., Farnsborough, England, 727/750.

14. J. Mikielewicz, J.R. Moszynski, "Minimum Thickness of a Liquid Film Flowing Vertically Down a Solid Surface," Int. J. Heat and Mass Transfer, 19, 1976, p. 771-776.

15. H. Brauer, "Strömung und Wärmeübergang bei Rieselfilmen," V.D.I. (Ver. Deut. Ingr.) - Forschungheft, 1956, p. 457.

V_s / m/s	Symmetric		Non-Sym	
	λ mm	σ	λ mm	σ
54.3	1.92	0.380	8.48	0.382
79.3	1.28	0.0834	7.40	1.66
129.6	1.36	0.0940	7.14	1.31
220.5	0.573	0.0310	5.65	1.60
302			4.21	1.38

λ ; MEAN VALUE OF WAVELENGTH

σ ; STANDARD DEVIATION of EACH WAVELENGTH

$$\sigma = \frac{1}{n-1} \sqrt{\sum_{i=1}^{n} (x_i - M)^2}$$

Table 1. The Average Wave Lengths and Standard Deviations.

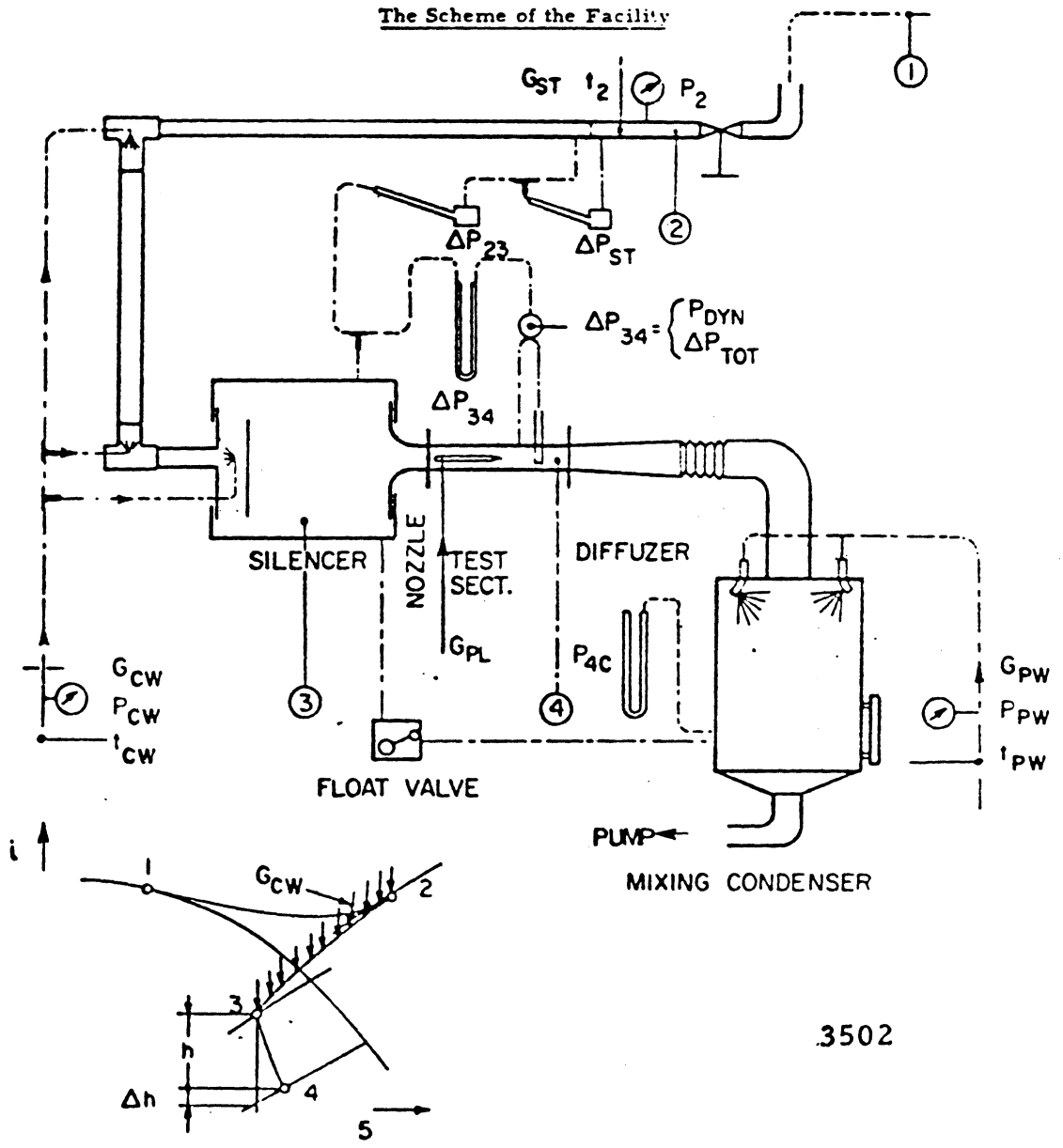

Figure 1 - Schematic Diagram of the University of Michigan Steam Tunnel (4)

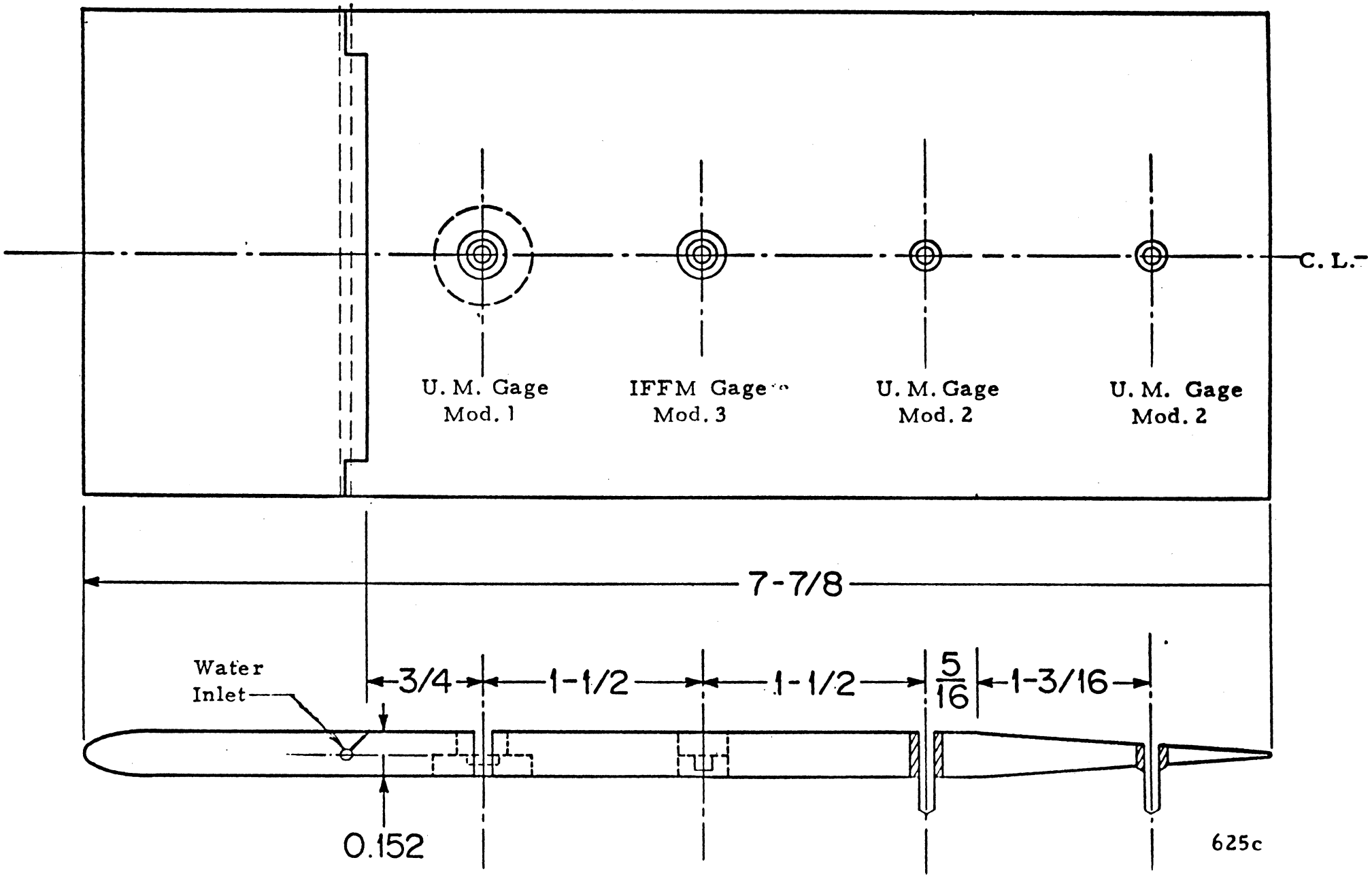

Figure 2 - Schematic of Blade with Gases

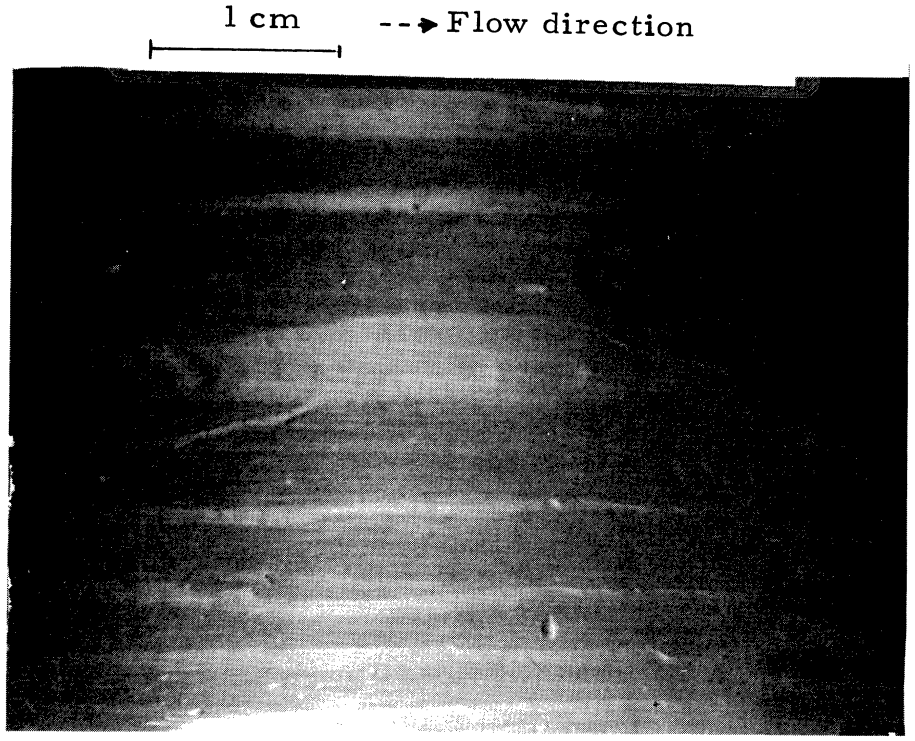

853a

Fig. 3 Dry Patches V_s=79 m/s q=5/8 cm^3/cm-min.

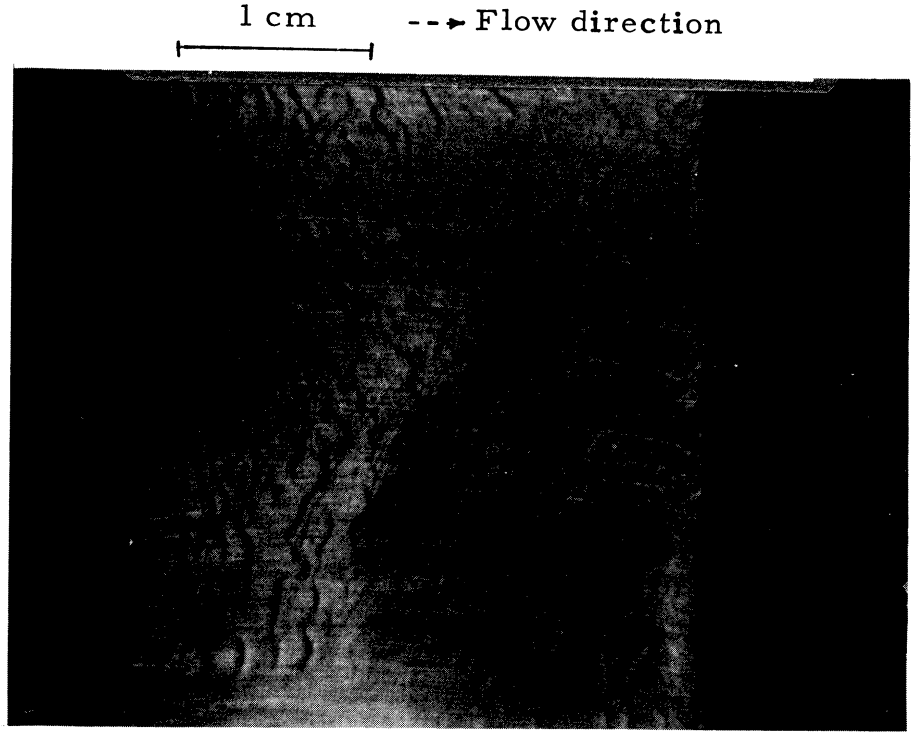

853b

Fig. 4 Symmetric Waves V_s=130 m/s q=15/16 cm^3/cm-min.

1 cm ---→Flow direction

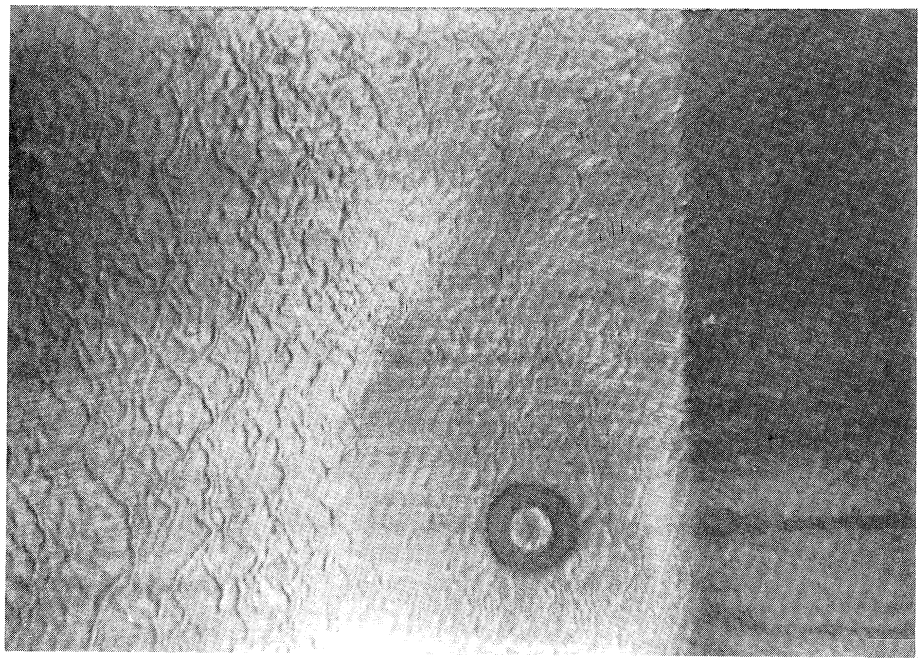

Fig. 5 Symmetric Waves V_s=200m/s $\dot{q}$=15/16 cm^3/cm-min.

1 cm ---→Flow direction

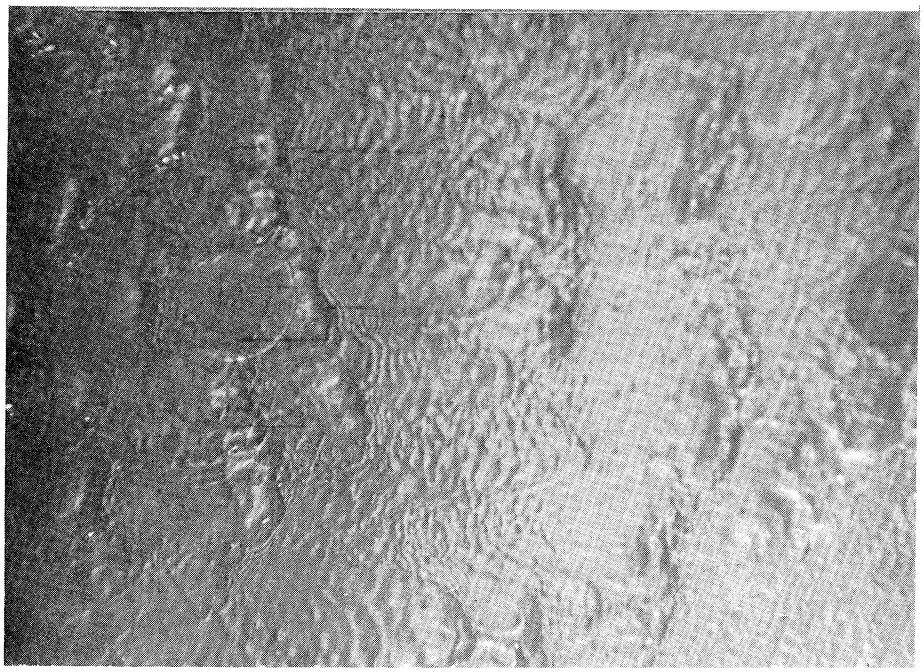

Fig. 6 Non-Symmetric Waves V_s=54 m/s $\dot{q}$=7.5 cm^3/cm-min.

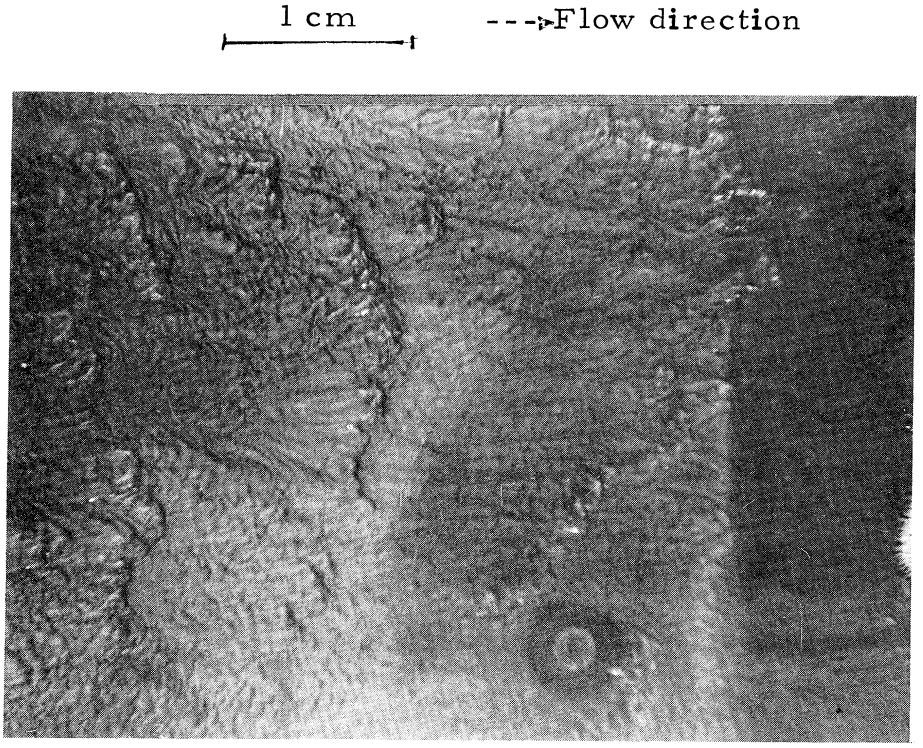

Fig. 7 Non-Symmetric Waves V_s=130 m/s $\dot{q}$=7.5 cm^3/ cm-min.

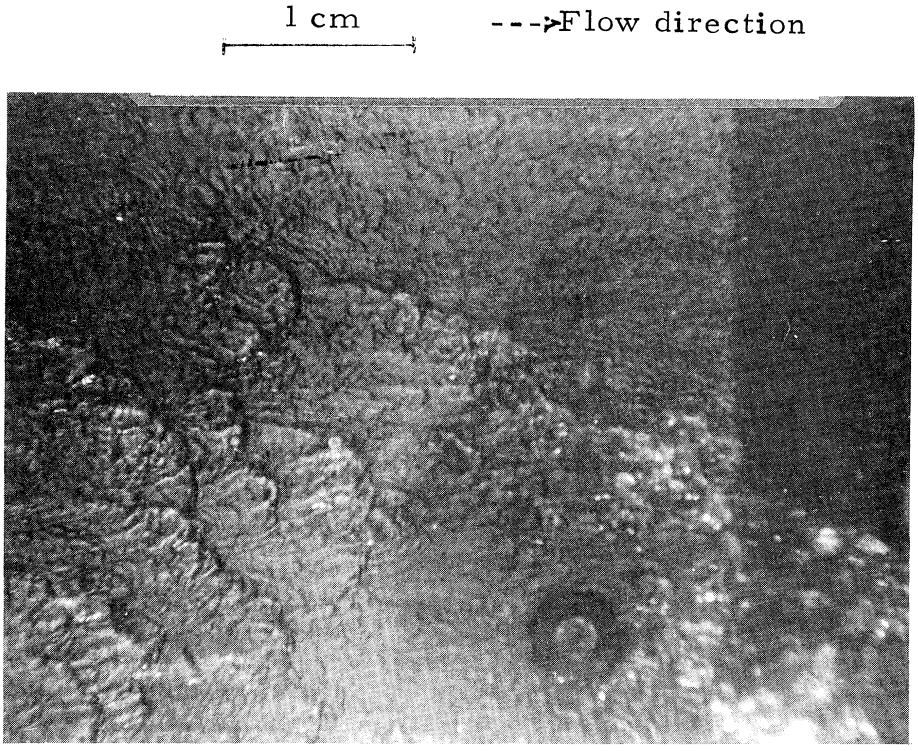

Fig. 8 Non-Symmetric Waves V_s=130 m/s q=10 cm^3/cm-min.

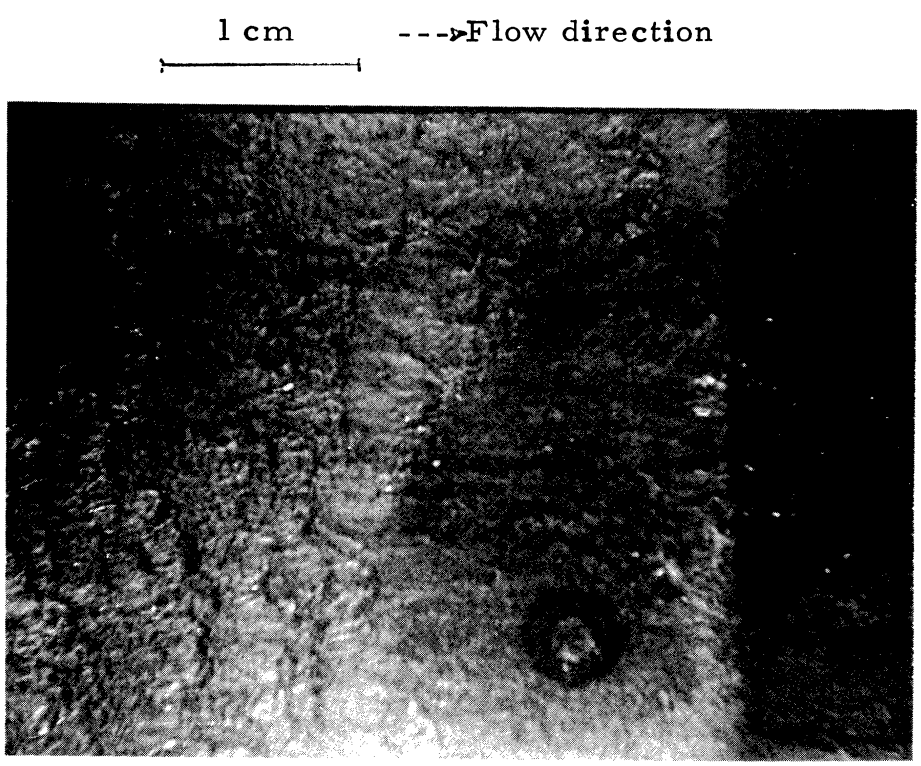

856a

Fig. 9 Film Breakup and Shedding V_s=221 m/s $\dot{q}$=15/16 cm^3/cm-min.

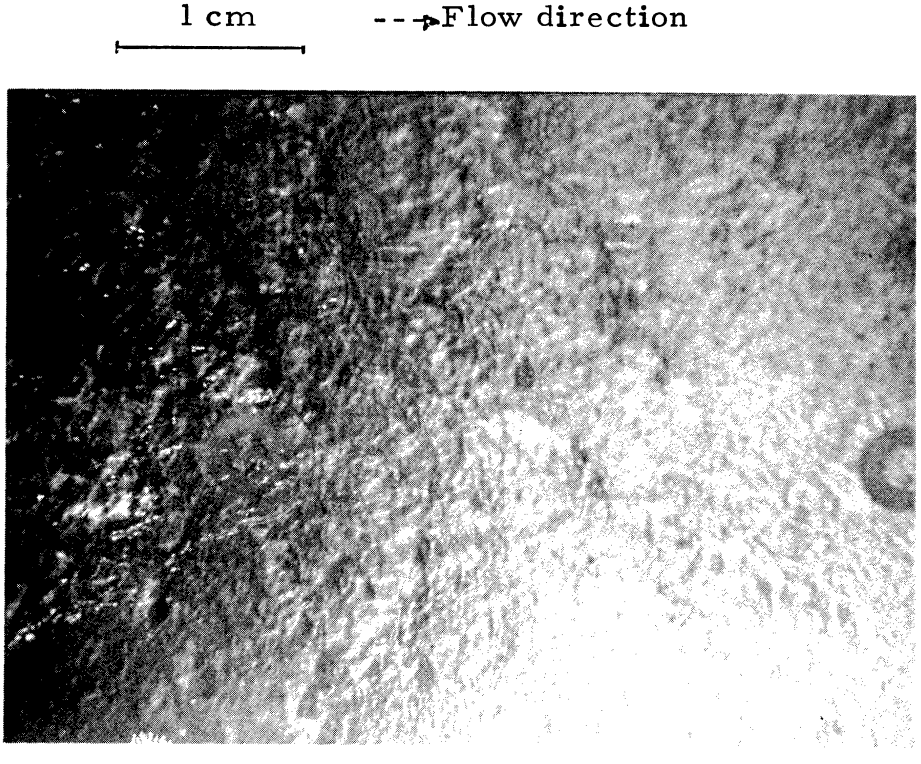

856b

Fig. 10 Film Breakup and Shedding V_s=221 m/s $\dot{q}$=1.25 cm^3/cm-min.

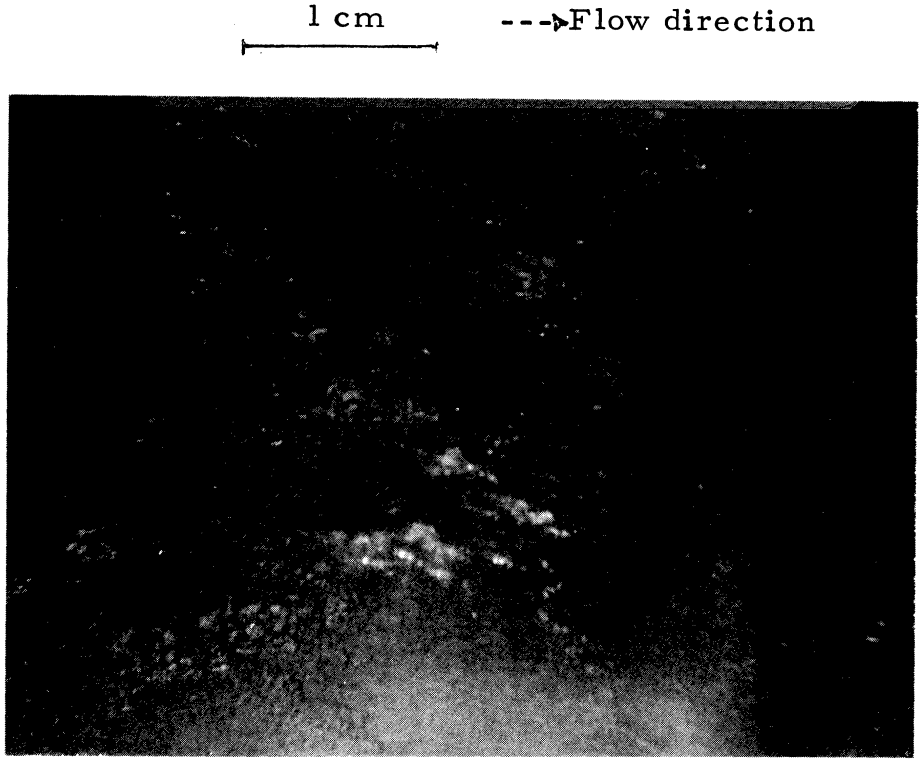

857

Fig. 11. Film Breakup and Shedding V_s=302 m/s $\dot{q}$=12.5 cm^3/cm-min.

PLOT OF WAVELENGTH VS. FLOW RATE.

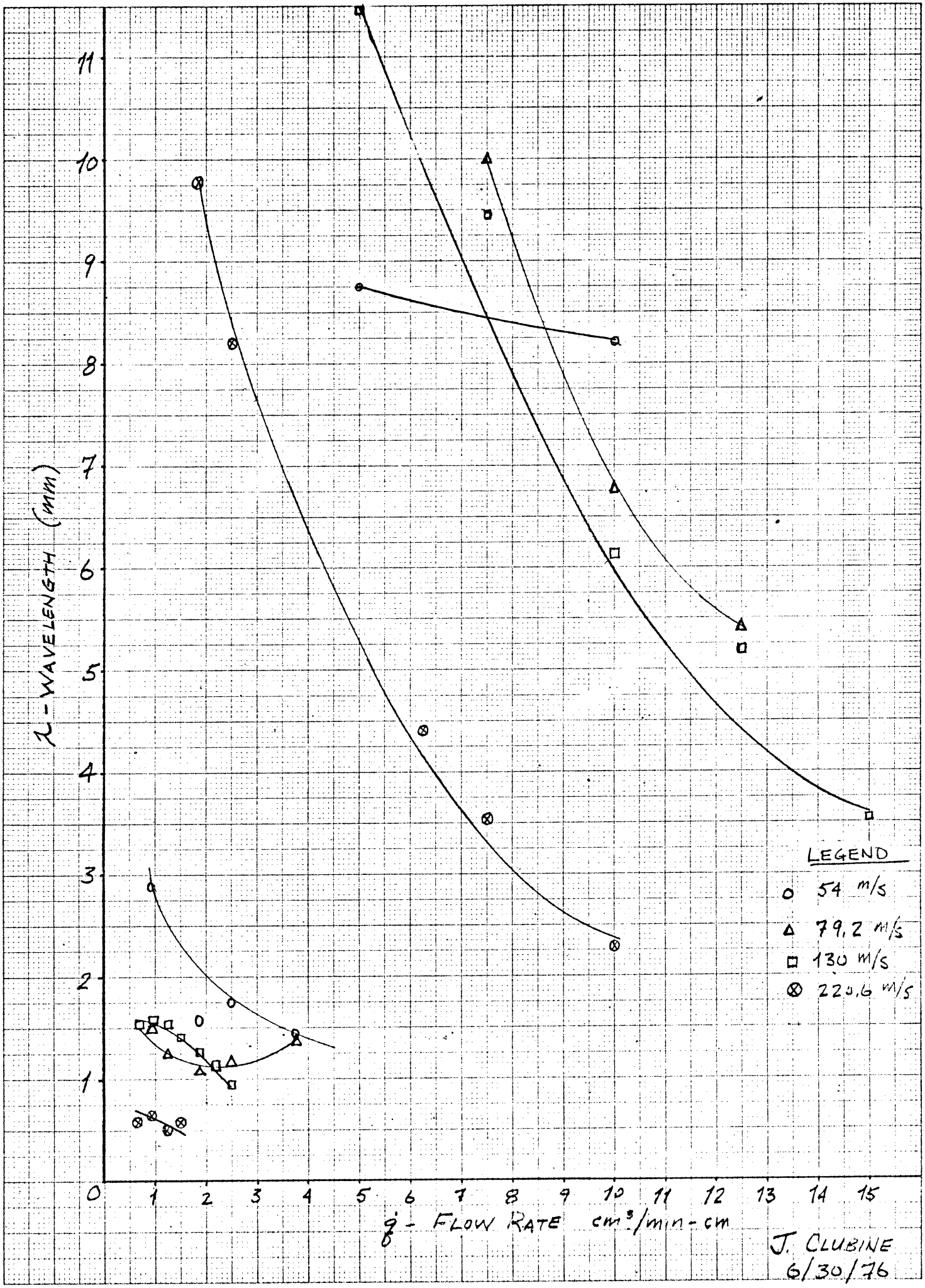

eters to the Centim

Fig 12 Wave Lengths vs. Flow Rate.

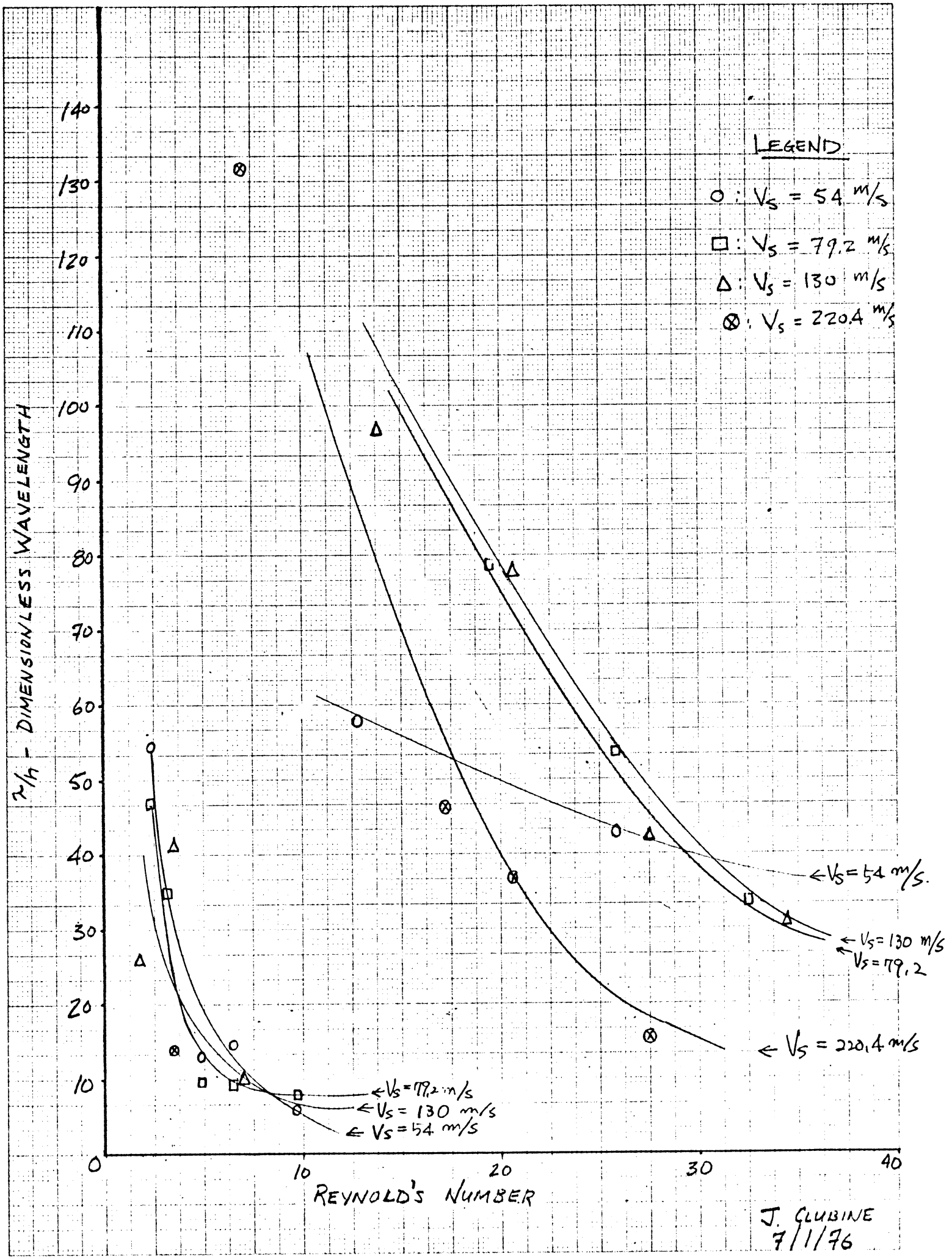

Fig 13 Dimensionless Wave Length Vs Reynolds Number.

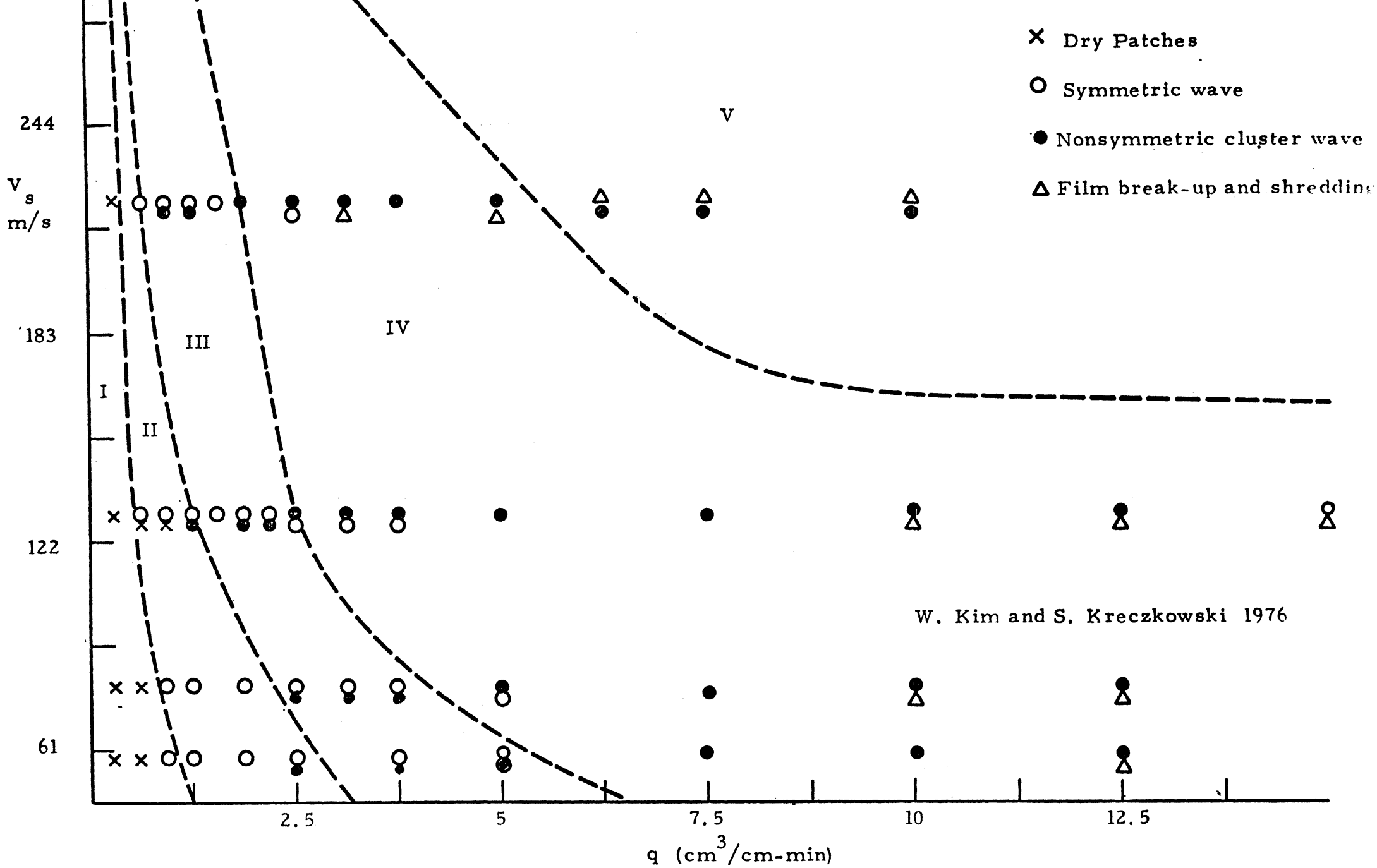

Fig. 14 Transition Map of Liquid Film and Steam Flow

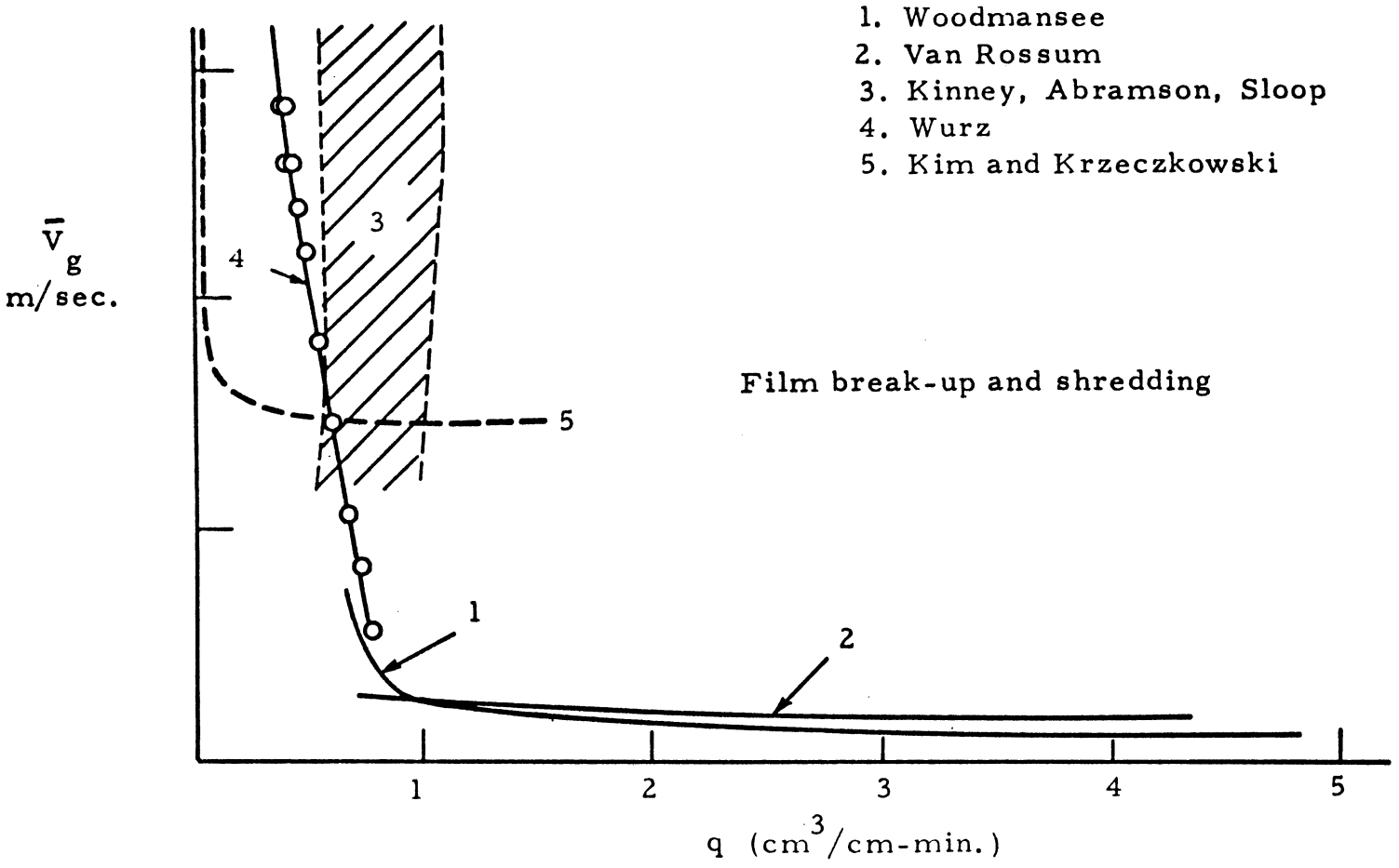

Fig. 15 Transition Line for Film Break-up

UNIVERSITY OF MICHIGAN
3 9015 03023 0364